GDCh Research Article Angewandte International Edition Chemie www.angewandte.org

How to cite: *Angew. Chem. Int. Ed.* **2025**, *64*, e202422459
doi.org/10.1002/anie.202422459

Protein Cages

High-Fidelity In Vitro Packaging of Diverse Synthetic Cargo into Encapsulin Protein Cages

Taylor N. Szyszka, Rezwan Siddiquee, Alex Loustau, Lachlan S. R. Adamson, Claire Rennie, Tiancheng Huang, Reginald Young, Andrew Care, and Yu Heng Lau**

Abstract: Cargo-filled protein cages are powerful tools in biotechnology with demonstrated potential as catalytic nanoreactors and vehicles for targeted drug delivery. While endogenous biomolecules can be packaged into protein cages during their expression and self-assembly inside cells, synthetic cargo molecules are typically incompatible with live cells and must be packaged in vitro. Here, we report a fusion-based in vitro assembly method for packaging diverse synthetic cargo into encapsulin protein cages that outperforms standard in cellulo assembly, producing cages with superior uniformity and thermal stability. Fluorescent dyes, proteins and cytotoxic drug molecules can all be selectively packaged with high efficiency via a peptide-mediated targeting process. The exceptional fidelity and broad compatibility of our in vitro assembly platform enables generalisable access to cargo-filled protein cages that host novel synthetic functionality for diverse biotechnological applications.

Introduction

Cages constructed from self-assembling proteins are ubiquitous in nature, providing a rich source of engineerable molecular scaffolds for biotechnological applications.[1,2] The most common class of engineered cages are virus-like particles (VLPs), formed when viral capsid proteins are assembled into hollow compartments in the absence of the viral genome.[3–5] Other commonly engineered cages include iron-storing ferritins,[6,7] de novo designed cages,[8] cage-forming enzymes such as lumazine synthase,[9] and prokaryotic proteinaceous organelles that include bacterial microcompartments[10,11] and encapsulin nanocompartments.[12,13] Each class of cage-forming proteins has distinct properties –, e.g., size, thermal and chemical stability, tolerance to sequence and cargo engineering, immunogenicity – determining their suitability across diverse applications that include targeted delivery vehicles for synthetic drug molecules, vaccine scaffolds for antigen display and catalytic nanoreactors for biomanufacturing.

The ability to package synthetic cargo into protein cages is a crucial limitation for many biotechnological applications. Protein cages typically assemble during their expression inside a cellular host, thus limiting cargo packaging to biomolecules that can be produced inside cells (Figure 1a). Indeed, we and many others have shown that protein cages can be readily reprogrammed to package cargo proteins or nucleic acids during assembly inside cells.[14–21] To load synthetic non-biological cargo however, protein cages are often purified from their cellular hosts, disassembled under buffer conditions that disfavour assembly (e.g., changing pH, ionic strength, temperature or adding chemical denaturants), then reassembled in the presence of the cargo.[22–31] Drawbacks of this approach include the risk of damage to cage proteins or cargo during exposure to potentially harsh disassembly conditions, as well as suboptimal cargo loading efficiency when a passive statistical encapsulation mechanism is used.[32–37] Furthermore, the subsequent in vitro reassembly process can have poor fidelity, generating

[*] T. N. Szyszka, R. Siddiquee, A. Loustau, L. S. R. Adamson, T. Huang, R. Young, Y. H. Lau
School of Chemistry, The University of Sydney, Camperdown, NSW 2006, Australia
E-mail: taylor.szyszka@sydney.edu.au
yuheng.lau@sydney.edu.au

T. N. Szyszka, R. Siddiquee, Y. H. Lau
The University of Sydney Nano Institute, The University of Sydney, Camperdown, NSW 2006, Australia

T. N. Szyszka, R. Siddiquee, L. S. R. Adamson, A. Care, Y. H. Lau
ARC Centre of Excellence in Synthetic Biology, The University of Sydney, Camperdown, NSW 2006, Australia

C. Rennie, A. Care
School of Life Sciences, University of Technology Sydney, Sydney, NSW 2007, Australia

C. Rennie
Australian Institute for Microbiology and Infection, Sydney, NSW 2007, Australia

Y. H. Lau
ARC Centre of Excellence for Innovations in Peptide and Protein Science, The University of Sydney, Camperdown, NSW 2006, Australia

Additional supporting information can be found online in the Supporting Information section

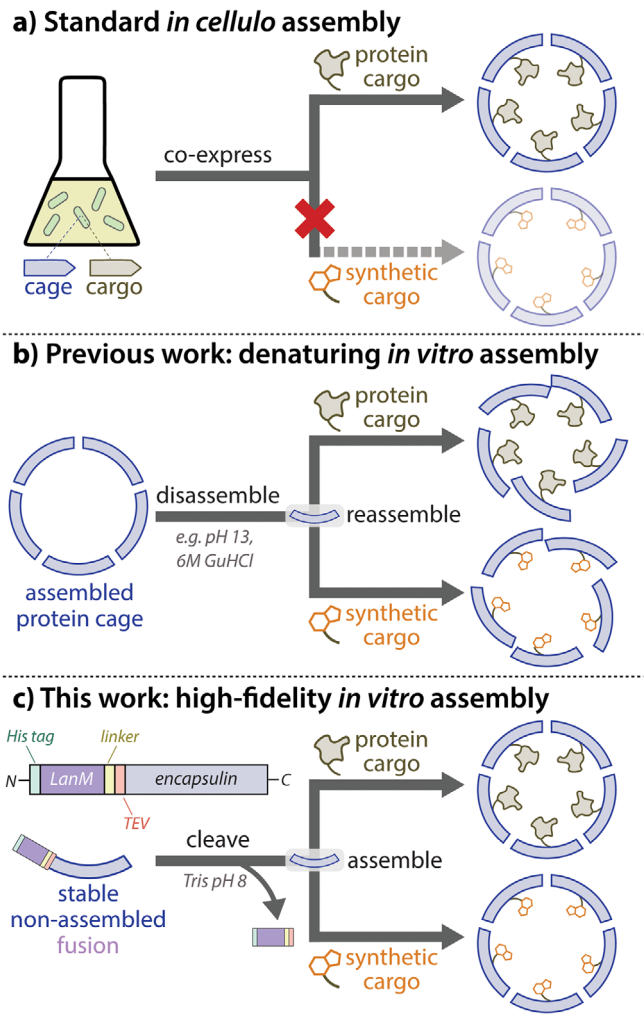

Figure 1. Strategies for packaging cargo into protein cages. a) Cargo packaging typically occurs in cells, where cargo that can be produced inside cells (proteins, nucleic acids) is packaged during the expression and assembly process. This method is generally incompatible with synthetic non-biological cargo. b) Current methods for in vitro packaging of synthetic cargo require cages to be disassembled then subsequently reassembled in the presence of cargo, which can lead to significant assembly defects and aggregation. c) We report a fusion-based strategy for triggering in vitro assembly in encapsulin protein cages, producing highly uniform and thermostable cages that can be loaded with diverse synthetic cargo.

a significant proportion of defective or aggregation-prone cages with inferior structural integrity, uniformity and thermal stability relative to their original correctly assembled native state.[22,23,38,39]

In this work, we report the high-fidelity in vitro packaging of diverse synthetic cargo into encapsulin protein cages. Encapsulins are simple non-viral protein cages with exceptional stability and a native peptide-mediated mechanism for loading proteinaceous cargo,[12] serving as ideal candidates for engineering drug delivery vehicles,[40–42] vaccine scaffolds[40,43] and nanoreactors.[14,44] Until now, the ability to package synthetic cargo into encapsulin cages in vitro has been challenging, as fully assembled encapsulins are not sufficiently porous to permit entry of larger molecular cargo.[16,45] Previously reported protocols for in vitro packaging require exposure to extreme buffer conditions (e.g., pH 1, pH 13 or 7 M GuHCl) for cage disassembly,[46] leading to low-yielding reassembly with substantial cage defects and aggregation (Figure 1b).[22,23] Here, we achieve in vitro assembly and cargo packaging by using a protein fusion strategy to circumvent the need for disassembly (Figure 1c). This strategy outperforms current in cellulo assembly and in vitro disassembly-reassembly methods for encapsulins, producing cargo-filled cages with superior uniformity and thermostability.

Results

LanM-QtEnc Is a Stable Fusion Protein That Does Not Readily Self-assemble into Native Cages

To engineer a stable pre-assembly form of encapsulin, we fused the 12 kDa lanthanide-binding protein lanmodulin (LanM) to the internally facing *N*-terminus of the 32 kDa encapsulin protein from *Quasibacillus thermotolerans* (QtEnc). We chose QtEnc as it natively forms the largest known encapsulin protein cage, consisting of 240 protomers with an external diameter of 42 nm,[47] while we chose LanM as the fusion partner due to its disordered structure (in the absence of lanthanides),[48] potentially serving as a dynamic steric blockade to prevent the self-assembly of QtEnc. We fused the two proteins via a flexible glycine-serine linker (GGSGGS) and a tobacco etch virus (TEV) protease cleavage site, allowing for removal of the LanM fusion as a trigger for assembly. Finally, we included a hexahistidine tag and GGS linker at the *N*-terminus of LanM to facilitate purification. The resulting 46 kDa fusion protein is henceforth referred to as LanM-QtEnc (Figure 1c).

Upon recombinant production in *Escherichia coli*, we found that LanM-QtEnc is a stable fusion protein that does not self-assemble into cages. Purification of LanM-QtEnc involved an initial affinity chromatography step over Ni-NTA resin, followed by size-exclusion chromatography (SEC) on a Superdex 200 column to yield the pure fusion protein as determined by SDS-PAGE analysis (Figure 2a). Subsequent blue native PAGE (BN-PAGE) analysis showed that LanM-QtEnc predominantly forms a single low molecular weight species, in contrast to the expected 8 MDa cage from in cellulo assembly, which is henceforth referred to as wild-type QtEnc (Figure 2b). Attempts to visualise the protein by negative-stain transmission electron microscopy (TEM) were consistent with a lack of assembled cage-like structures (Figure S1a).

We used analytical SEC to confirm that LanM-QtEnc exists in a predominantly unassembled form. SEC was performed on two different columns to achieve sufficient separation across a broad size range. Separation on a Superose 6 Increase column 10/300 GL (5–5000 kDa) showed a clear difference between wild-type QtEnc and LanM-QtEnc (Figure 2c), with the wild-type cage eluting early in the unretained peak, and the fusion eluting 9 mL later, near the end of the chromatograph. Meanwhile, a Bio SEC-5 HPLC

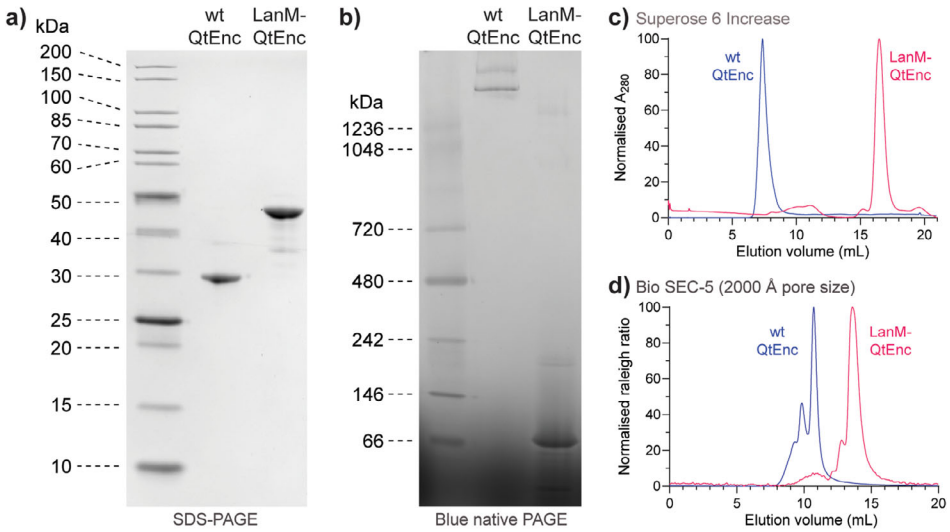

Figure 2. LanM-QtEnc is an encapsulin fusion that does not self-assemble into cages. a) SDS-PAGE analysis of purified wild-type QtEnc and LanM-QtEnc fusion shows the expected protein bands at 32 and 46 kDa, respectively. b) Blue native PAGE analysis of LanM-QtEnc shows that the fusion exists predominantly in a low molecular weight form, while wild-type QtEnc forms the expected high molecular weight assembly, along with a faint smeared band corresponding to other potentially aberrant assemblies. c) Size-exclusion chromatography on a Superose 6 Increase 10/300 GL column confirms that LanM-QtEnc exists in an unassembled state, distinct from the cage assembly formed by wild-type QtEnc. d) Size-exclusion chromatography with light scattering detection on a Bio SEC-5 2000 Å HPLC column provides sufficient resolution and sensitivity at the megadalton size range to provide further evidence of aggregated or misassembled species in wild-type QtEnc.

column with 2000 Å pore size (maximum mass range > 10 MDa) also showed a substantial difference in retention time (Figure 2d), using light scattering in place of UV absorbance to enhance detection sensitivity at analytical scale. Notably for wild-type QtEnc, we also observed the presence of two additional peaks with earlier retention times (Figure 2d), indicating the existence of aggregated or misassembled cages that likely formed as a result of recombinant overexpression in *E. coli*. This polydisperse behaviour has not previously been reported for QtEnc in the literature due to limited resolving range of analytical SEC columns used in prior studies,[23,47] although published dynamic light scattering (DLS) measurements suggest the existence of larger species (47.2 nm average diameter reported, 42 nm expected based on cryo-EM).[49]

Cages Assembled In Vitro Upon Fusion Cleavage Are More Uniform and Stable than Cages Assembled In Cellulo

We observed the high-fidelity in vitro assembly of encapsulin cages upon cleavage of the LanM-QtEnc fusion with TEV protease. SEC analysis on the Bio SEC-5 HPLC column revealed that the in vitro assembled cages were more uniform than wild-type QtEnc assembled in *E. coli*, forming a single species with a calculated mass of 8.2 ± 0.2 MDa from multi-angle light scattering (MALS) measurements (Figures 3a and S1b). Encapsulin cages were isolated post-cleavage by SEC on a Superose 6 Increase 10/300 GL column, eluting in the unretained peak as expected for a large 8 MDa assembly (Figure 3b). BN-PAGE analysis provided further confirmation of the clean and complete conversion to an assembled state (Figure 3c), while SDS-PAGE analysis showed that cleavage had proceeded to > 95% completion based on gel densitometry (Figure 3d).

The successful assembly of uniform cages was confirmed by negative stain TEM (Figure 3e) with the expected diameter of 42 nm calculated from hydrodynamic radius (20.8 ± 0.7 nm) by DLS measurements (Figure 3f). The 50 nm diameter calculated for wild-type QtEnc by DLS provided further evidence of non-uniformity for assemblies produced in *E. coli*. Notably, unexpected diameters have been observed by DLS in previous attempts to disassemble and re-assemble encapsulins in vitro using denaturants, base, and heat,[23] as well as in vitro studies on an engineered pH-switchable version of QtEnc,[49] both of which were attributed to some degree of misassembly or aggregation.

The in vitro assembled cages showed exceptional thermal stability that exceeded that of the wild-type QtEnc assembled in *E. coli*. The melting temperature (T_m) of the in vitro assemblies was 100°C by differential scanning fluorimetry (DSF), compared to 55.9°C for the LanM-QtEnc fusion prior to cleavage (Figure 3g). Meanwhile, wild-type QtEnc had a T_m of 84.4°C, consistent with equivalent data from Giessen et al.[47] This increased thermal stability implies a lower rate of aggregation and misassembly and therefore qualitatively higher fidelity in the case of in vitro cage assembly, though further structural analyses would be required for a quantitative interpretation.

Protein Cargo and Synthetic Molecules Can be Selectively and Efficiently Packaged during In Vitro Assembly

To demonstrate that the native cargo packaging system of encapsulins was functional in vitro, we encapsulated

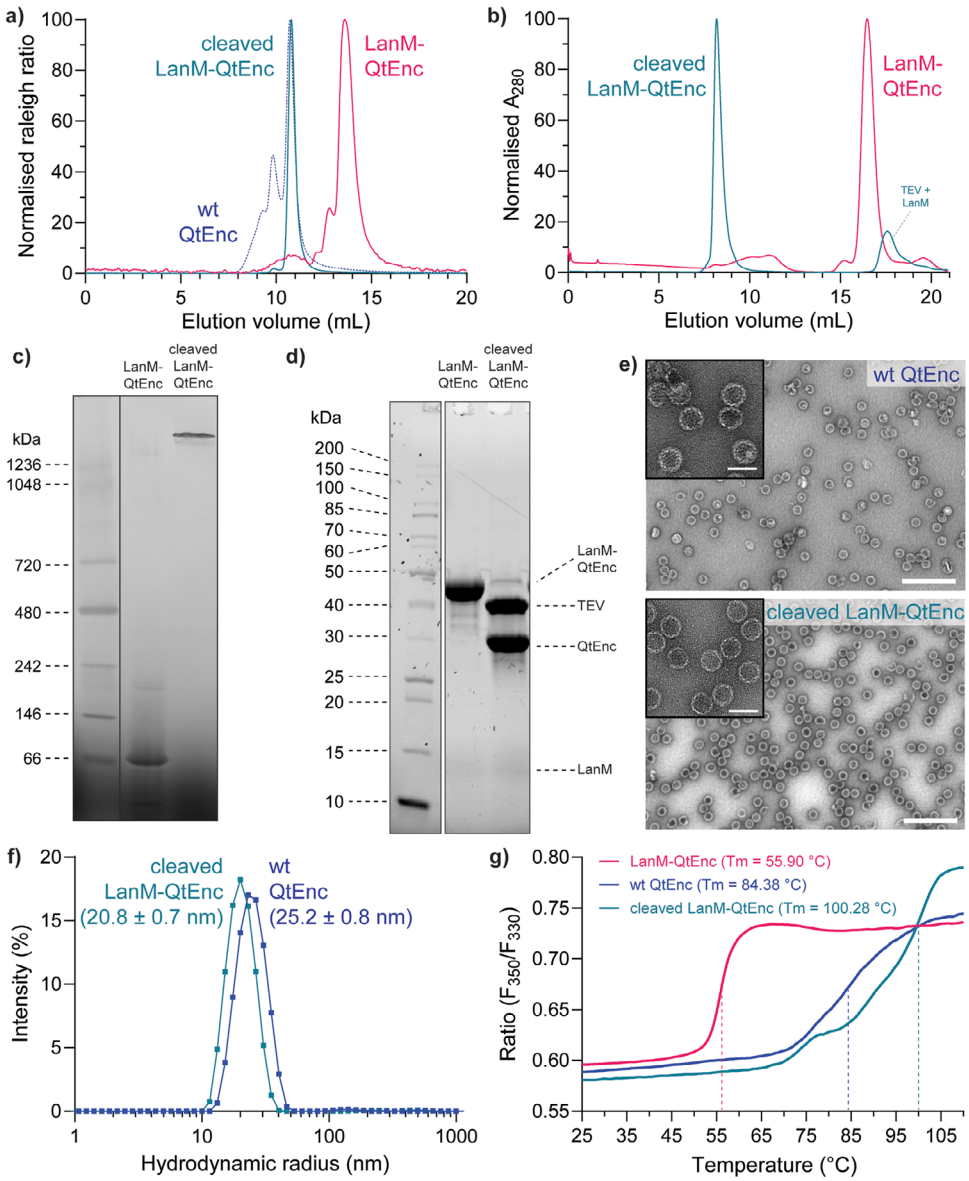

Figure 3. LanM-QtEnc cleavage triggers high-fidelity assembly of encapsulin cages. a) Analytical size-exclusion chromatography of the crude cleavage mixture on a Bio SEC-5 2000 Å HPLC column shows that the in vitro assembled encapsulins are highly monodisperse (92% by peak integration), with the peak eluting at 11 mL, without any of the additional peaks observed for wild-type QtEnc assembled in *E. coli* (53% by peak integration). b) Size-exclusion chromatography purification on a Superose 6 Increase 10/300 GL column shows clean conversion to a high molecular weight species. c) Blue native PAGE analysis of the purified in vitro assembled encapsulins indicates clean and quantitative conversion to a high molecular weight species. d) SDS-PAGE of the crude cleavage mixture shows that cleavage proceeded to > 95% completion. e) Negative stain transmission electron microscopy of in vitro assembled encapsulins shows particles with similar cage morphology and size to wild-type QtEnc. The primary images were obtained at 40 000 × magnification (scale bar = 250 nm), while the inset images were obtained at 200 000 × magnification (scale bar = 50 nm). f) Dynamic light scattering measurements show that in vitro assembled encapsulins formed cages with a radius of ~21 nm (PDI 0.13 ± 0.03), consistent with a 42 nm diameter as stated in the literature, while wild-type QtEnc was slightly larger at a radius of ~25 nm (PDI 0.16 ± 0.04) due to the presence of minor aggregates or misassembled structures. g) Differential scanning fluorimetry shows that in vitro assembled encapsulins are more thermostable than wild-type QtEnc assembled in *E. coli*. DLS and nanoDSF measurements were conducted across two biological replicates, each with ten technical replicates.

fluorescent protein mNeonGreen with the specific cargo loading peptide (CLP) for *Q. thermotolerans* encapsulin fused to the C-terminus (mNeon-Qt) (Figure 4a). The negative control for cargo packaging was the analogous mNeonGreen construct fused to the CLP for *T. maritima* encapsulin (mNeon-Tm), which does not mediate cargo packaging when co-expressed with QtEnc in *E. coli*.[14] mNeon-Qt or mNeon-Tm was added during TEV cleavage of LanM-QtEnc, using a 1:10 molar ratio of cargo:encapsulin to avoid the possibility of sterically-induced defects arising from cargo overloading.[50] After in vitro assembly, Ni-NTA resin was used to remove His-tagged species including TEV protease,

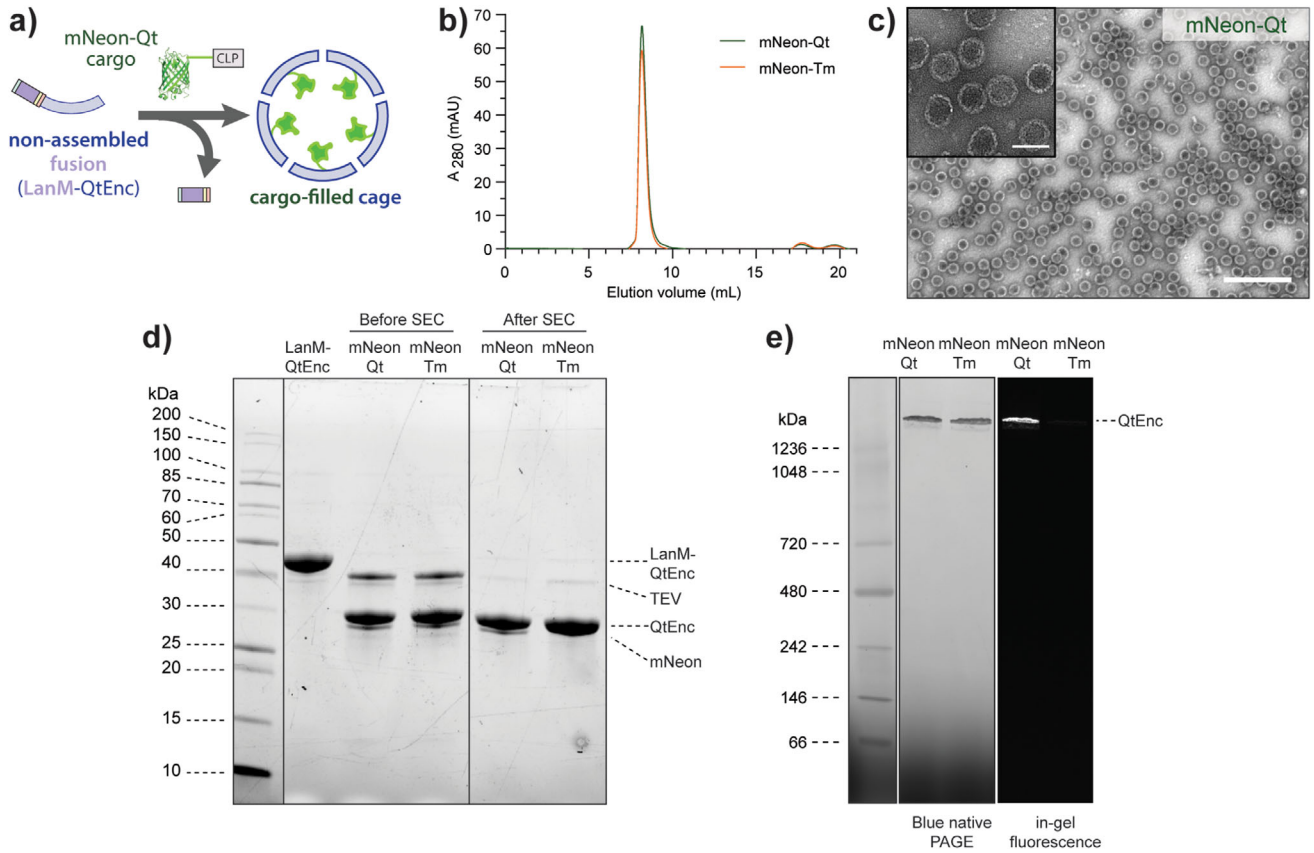

Figure 4. Selective packaging of protein cargo during in vitro assembly. a) Schematic of mNeon-Qt packaging into encapsulin by triggered in vitro assembly. b) Size-exclusion chromatography on a Superose 6 Increase 10/300 GL column shows that in vitro assembly is unaffected by the presence of cargo. c) Negative stain transmission electron microscopy of in vitro packaged encapsulin cages have similar morphology and size to wild-type QtEnc. The larger images were taken at 40 000 × magnification (scale bar = 250 nm), while the inset images were taken at 200 000 × magnification (scale bar = 50 nm). d) SDS-PAGE analysis of LanM-QtEnc cleavage in presence of cargo before and after SEC purification on a Superose 6 Increase 10/300 GL column. mNeon-Qt co-elutes with QtEnc cages while mismatched mNeon-Tm is not visible on the gel. e) Blue native PAGE analysis shows clear in-gel fluorescence for in vitro assemblies containing mNeon-Qt protein cargo, while fluorescence is not visible for mNeon-Tm indicating that it was not packaged.

cleaved LanM, and any potentially unencapsulated mNeon cargo. SEC purification on a Superose 6 Increase 10/300 GL column showed that the efficiency of in vitro assembly was unaffected by the presence of cargo (Figure 4b), while negative stain TEM imaging confirmed the presence of uniform assemblies (Figure 4c). SDS-PAGE analysis showed that only mNeon-Qt co-eluted with the in vitro assembled encapsulins (Figure 4d), and BN-PAGE analysis confirmed that mNeon-Qt was selectively packaged into cages while mNeon-Tm was not packaged (Figure 4e). Unencapsulated mNeon-Qt was not observed during SEC purification (Figure S2), and absorbance measurements on purified mNeon-filled cages for total protein at 280 nm and mNeon-Qt cargo at 506 nm confirmed that mNeon-Qt had been packaged with minimal loss of cargo with approximately 20 molecules of mNeon per encapsulin shell (Figure S3).

Next, we showed that synthetic small molecules can be packaged in vitro (Figure 5a). The synthetic fluorescent dye 5-carboxytetramethylrhodamine (TMR) was attached to the *N*-terminus of the CLPs for *Q. thermotolerans* (TMR-Qt) and *T. maritima* (TMR-Tm) by Fmoc solid-phase peptide synthesis. The in vitro cargo loading experiments were repeated with TMR in place of mNeonGreen and using Capto Core 700 resin in place of Ni-NTA resin after assembly to remove TEV protease, cleaved LanM, and any potentially unencapsulated cargo. Once again, the presence of synthetic cargo did not affect the fidelity and efficiency of assembly according to analytical SEC (Figure 5b) and TEM (Figure S4). In-gel fluorescence was observed after conducting BN-PAGE on purified cages in vitro loaded with TMR-Qt, confirming successful and specific encapsulation of the synthetic dye, while no fluorescence was observed for the TMR-Tm negative control (Figures 5c and S5).

To expand the scope of cargo packaging beyond proteins and synthetic dyes, we packaged the synthetic drug molecule aldoxorubicin (Aldox), a maleimide-functionalised prodrug form of the chemotherapeutic doxorubicin (Dox) (Figure 5d). Aldox was conjugated onto a Cys-modified Qt CLP to generate Aldox-Qt, while free Dox was used as a negative control. Both Aldox-Qt and free Dox were in vitro packaged in a 2:1 molar ratio of encapsulin to cargo. This higher ratio of cargo packaging was chosen as it was expected to provide sufficient photophysical signal for detection given the reduced brightness of Aldox relative to

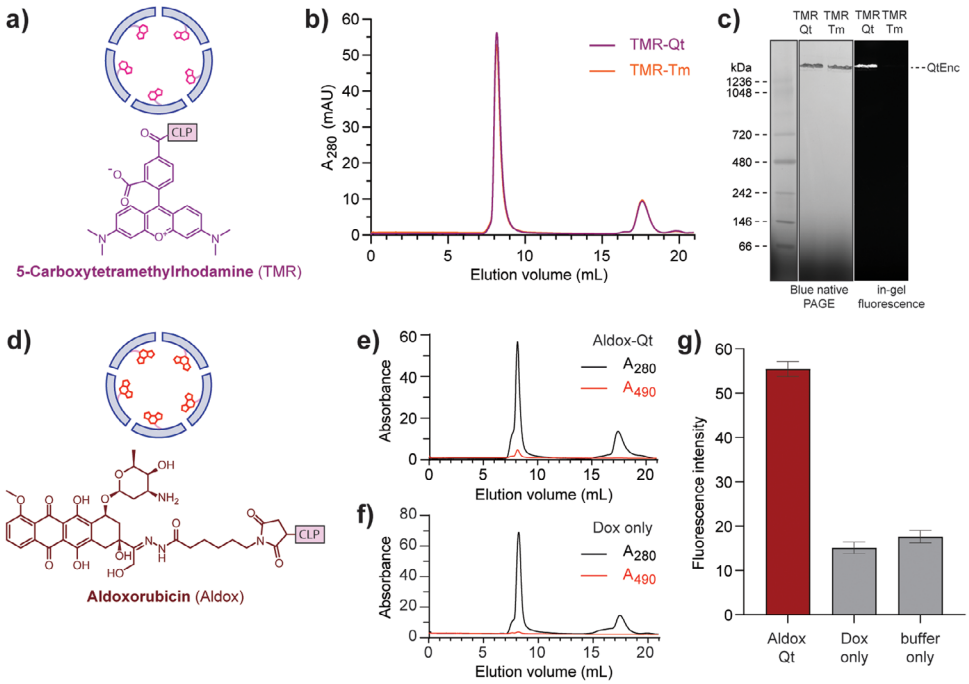

Figure 5. In vitro packaging of diverse synthetic cargo into encapsulin cages. a) Schematic of TMR-Qt in vitro packaged into encapsulin cages. b) Size-exclusion chromatography monitoring absorbance at 280 nm on a Superose 6 Increase 10/300 GL column shows that the fidelity of in vitro assembly is unaffected by the presence of TMR cargo. c) Blue native PAGE analysis shows clear in-gel fluorescence for in vitro assemblies with TMR-Qt synthetic cargo selectively packaged, while fluorescence is not visible for TMR-Tm. d) Schematic of Aldox-Qt in vitro packaged into encapsulin cages. e,f) Size-exclusion chromatography monitoring absorbance at 490 nm on a Superose 6 Increase 10/300 GL column suggests that Aldox-Qt co-elutes with encapsulin assemblies, while doxorubicin without the CLP does not co-elute with encapsulin. g) Fluorescence intensity of the encapsulin fractions from SEC purification show aldoxorubicin fluorescence (emission at 595 nm) when Aldox-Qt is packaged, while the negative control of packaging doxorubicin without the CLP only shows background levels of fluorescence. Error bars correspond to the standard error of the mean across 100 technical measurement replicates.

the previously packaged fluorophores, while avoiding cargo overloading defects. Analytical SEC on a Superose 6 Increase 10/300 GL column showed an Aldox-specific absorbance peak (490 nm) in the encapsulin fraction for in vitro packaged Aldox-Qt (Figure 5e,f). Furthermore, fluorescence emission was only observed in encapsulin samples purified after in vitro assembly with Aldox-Qt, while the negative control with free Dox showed equivalent signal to the buffer-only control (Figure 5g), further verifying that Aldox-Qt was selectively packaged. Taken together, these results show that diverse synthetic cargo can be efficiently packaged into encapsulins in vitro by taking advantage of the highly specific encapsulin-CLP interaction.

Synthetic Cargo Packaged within Encapsulins Can Be Delivered into Murine RAW 264.7 Cells

Encapsulins hold great promise for intracellular applications, such as drug delivery and intracellular catalysis. Uptake of modified encapsulin systems into macrophages has previously been shown and internalisation confirmed via fluorescence microscopy.[51,52] As such, we investigated whether in vitro assembled encapsulins could facilitate uptake of fluorescent mNeon-Qt and TMR-Qt cargo into live cells. Cellular uptake of packaged cargo into murine RAW 264.7 macrophage-like cells was assessed by confocal fluorescence microscopy. Intracellular fluorescence was readily observed in 83% of cells when encapsulated mNeon-Qt was added, with increased internalisation evident as bright punctate areas, which is not evident in macrophages treated with non-encapsulated mNeon-Qt (Figure 6a–c). Similarly, intracellular fluorescence was evident for packaged TMR-Qt in 50% of cells, while free TMR-Qt did not result in any fluorescence (Figure 6d–f). Bright punctate areas of internalised encapsulin suggests endocytosis and intracellular processing into early endosomes/endolysosomes, where the encapsulin shell may confer some protective effect to the fluorescent cargo. Once endocytosed, vesicles may fuse with acidified endosomal compartments to destroy pathogens[53,54]; however, Qt encapsulins have been shown to be very pH stable[23] and therefore may confer some protection from degradation. In summary, these results provide a proof of concept that in vitro assembled encapsulins can facilitate cellular uptake of cargo molecules.

Discussion

LanM-QtEnc is a novel protein construct that enables in vitro packaging of synthetic cargo into encapsulin cages, providing access to new biotechnological opportunities that cannot be explored using standard cell-based assembly approaches.

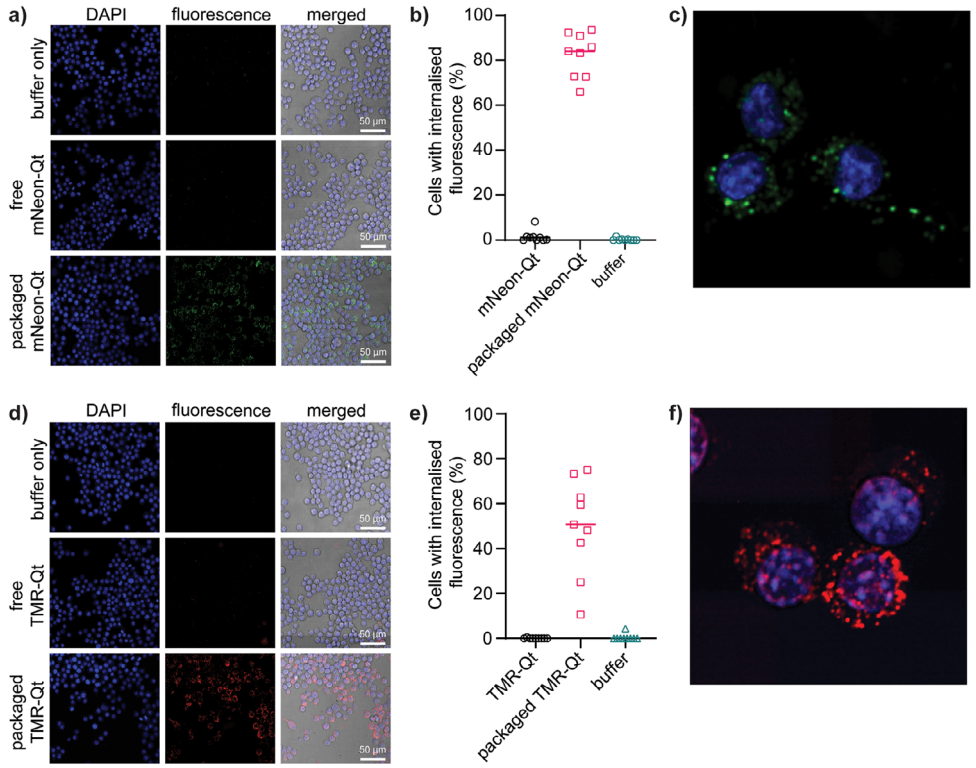

Figure 6. Cellular uptake of cargo in vitro packaged inside encapsulins. a) Confocal fluorescence microscopy images of murine RAW 264.7 cells with DAPI fluorescence (nuclear stain) and fluorescence in the FITC channel (mNeon). Merged indicates an overlay of the two channels, as well as brightfield imaging. In vitro packaged mNeon-Qt was observed inside cells while free mNeon-Qt was not observed. b) ImageJ quantification of fluorescence shows that a median of 83% of cells showed uptake of packaged mNeon-Qt, while minimal uptake was observed for free mNeon-Qt and buffer-only controls. Data analysis was performed on three independent fields of view from three biological replicates. c) Representative magnified image of RAW 264.7 cells showing intracellular localisation of packaged mNeon-Qt. d) Confocal microscopy images of RAW 264.7 cells with DAPI and fluorescence in the TRITC channel (TMR). In vitro packaged TMR-Qt was observed inside cells while free TMR-Qt was not observed. e) ImageJ quantification of fluorescence shows that a median of 50% of cells showed uptake of packaged TMR-Qt, while minimal uptake was observed for free TMR-Qt and buffer-only controls. Data analysis was performed on three independent fields of view from three biological replicates. f) Representative magnified image of RAW 264.7 cells showing intracellular localisation of packaged TMR-Qt.

In vitro packaging is necessary for any synthetic molecular cargo that is incompatible with living cells due to cytotoxicity, metabolic instability, or membrane impermeability. In applications where multiple cargo types are packaged simultaneously, in vitro packaging also provides the opportunity for far greater control over cargo stoichiometry than state-of-the-art genetic methods for tuning expression levels in cells.[55,56] Even in the case of biomolecular cargo that can be produced in cells, in vitro packaging solves any timing issues where cargo requires additional processing prior to packaging, such as any cargo that requires multiple subunits to form an active complex, or cargo that must undergo post-translational modification to be functional.

A distinctive feature of the LanM-QtEnc system is the exceptional fidelity of cage assembly and cargo packaging. Defective assembly pathways are commonly encountered during most in vitro assembly methods,[23,26,57–59] as well as in some in cellulo assembly methods.[60] Low-fidelity assembly processes result in defects or aggregates that can reduce the overall yield of desired cages, pose challenges for sample purification, and undermine the fundamental properties that make protein cages valuable in biotechnology. In nanoreactor design for example, protein cages can act as a semi-permeable barrier to control substrate flux and sequester toxic or unstable intermediates, or alternatively, act as a protective layer for fragile enzymatic cargo.[14,32,61–65] Assembly defects compromise the ability of cages to achieve both of these core functions. In drug delivery applications, heterogeneous formulations arising from defective cage assemblies may be less stable in vivo, and hence less effective in shielding cytotoxic payloads from non-specific release prior to reaching the site of action. In addition, cargo packaging efficiency is a critical parameter when working with valuable cargo where losses must be minimised.

The LanM-QtEnc fusion stands out as a unique example of a stable encapsulin construct that does not form a fully assembled cage. In most literature examples of encapsulin engineering, the assembled state of encapsulins is strongly favoured. Lee et al. have reported several *N*-terminal antimicrobial peptide fusion constructs to engineered versions of the 24 nm encapsulin from *T. maritima*, observing cage formation along with increased heterogeneity in most cases.[66] A notable native example of *N*-terminal encapsulin fusion that does not impede assembly is the encapsulin system from *Pyrococcus furiosus*, which has its cargo directly fused on the *N*-terminal interior of the cage.[67] The *N*-terminal

fusion behaviour of LanM-QtEnc also differs from the HK97 bacteriophage capsid protein (from which encapsulins derive their HK97-like protein fold), where the scaffold protein gp5 is initially fused to the capsid protein during the immature Prohead-I that can form a mix of cages and dissociated capsomeres, but then is cleaved to initiate maturation to the final Head II phage capsid form.[68]

While the robustness of assembled encapsulin cages is ideal for many biotechnological applications, this robustness has also posed a significant technical barrier for previously reported disassembly-reassembly protocols, necessitating extreme pH or chemical denaturants to attempt cargo loading with poor fidelity.[22,42] In one exception, Jessen-Trefzer and co-workers covalently conjugated synthetic small molecule cargo on the inside of encapsulin cages without any disassembly,[52] although larger cargo is expected to be excluded from accessing the cage interior due to the narrow pore size of most encapsulins. Meanwhile, Giessen and co-workers inserted a pH-sensitive GALA peptide into the encapsulin sequence to generate a dynamic switchable assembly, albeit with an unexpected increase in diameter suggesting possible heterogeneity (62.2–76.8 nm average diameter by DLS).[49] Unlike all these examples, LanM-QtEnc entirely circumvents the challenge by starting from a non-assembled state. More generally, the extreme buffer conditions required for encapsulin disassembly are not shared by all protein cages. Some VLPs are inherently capable of disassembly via relatively mild changes in experimental buffer conditions. VLPs of the brome mosaic virus coat protein can assemble at low pH and ionic strength but disassemble at neutral pH and high ionic strength,[69] while VLPs of polyomavirus capsid proteins such as SV40 VP1 can be isolated from cells as pentameric capsomeres and assembled with the addition of DNA.[70] As a trade-off however, these VLPs have inherently less tolerance to the wide range of non-native conditions required for different biotechnological applications.

Beyond encapsulins and VLPs, there has been recent surging interest in the in vitro assembly of other types of protein cages. In work on the *Haliangium ochraceum* microcompartment shell protein, Kerfeld and co-workers used a SUMO-fusion strategy for the in vitro assembly of tubes and cages, where SUMO fusion produced a soluble hexameric state and subsequent SUMO cleavage led to higher-order oligomeric assembly.[71] Hilvert and co-workers recently used a fusion of maltose-binding protein to achieve in vitro assembly of an engineered lumazine synthase cage that packages RNA,[72] while Podobnik and co-workers used this strategy to assemble hollow nanotubes based on the coat protein of potato virus Y.[73]

In addition to building nanoreactors and drug delivery systems based on in vitro assembly, there are multiple future avenues for deepening our fundamental understanding of the LanM-QtEnc fusion system. In future work, we will investigate the origins of LanM stabilisation of the non-assembled state, to determine whether LanM is indeed unique in this role and whether disorder of the fusion partner is a significant contributor. The packaging efficiency across a broad range of non-protein cargoes will also be explored. The impact of lanthanide binding to LanM on self-assembly and cage stability is another possible area of further investigation. Finally, we will investigate whether LanM fusion can be used on other encapsulins, including pore-engineered encapsulins, and potentially even more generally across other HK97-fold capsids and unrelated cages, ultimately leading to a diverse set of in vitro assembled protein cages for new biotechnological applications.

Supporting Information

The authors have cited an additional reference within the Supporting Information.[74]

Acknowledgements

Y.H.L. acknowledges funding from the Australian Research Council (DE19010062, DP230101045) and Westpac Scholars Trust (WRF2020). The authors acknowledge the core facilities at Sydney Analytical and Sydney Microscopy and Microanalysis for providing infrastructure support. T.N.S., R.S., L.S.R.A. and Y.H.L. acknowledge support from the ARC Centre of Excellence in Synthetic Biology, while Y.H.L. also acknowledges support from the ARC Centre of Excellence for Innovations in Peptide and Protein Science. A.C. acknowledges funding from the Dementia Australia Research Foundation; Mason Foundation; and the National Foundation for Medical Research and Innovation. The authors acknowledge the use of the Nikon A1 inverted confocal microscope in the Microbial Imaging Facility at AIMI in the Faculty of Science, the University of Technology Sydney.

Open access publishing facilitated by The University of Sydney, as part of the Wiley - The University of Sydney agreement via the Council of Australian University Librarians.

Conflict of Interests

T.N.S., R.S. and Y.H.L. are inventors of patents related to this work. The remaining authors declare no competing interests.

Data Availability Statement

The data that support the findings of this study are available from the corresponding author upon reasonable request.

Keywords: Drug delivery · Nanoreactor · Protein cage · Supramolecular chemistry · Synthetic biology

[1] T. G. W. Edwardson, M. D. Levasseur, S. Tetter, A. Steinauer, M. Hori, D. Hilvert, *Chem. Rev.* **2022**, *122*, 9145–9197.
[2] N. F. Steinmetz, S. Lim, F. Sainsbury, *Biomater. Sci.* **2020**, *8*, 2771–2777.
[3] B. Ikwuagwu, D. Tullman-Ercek, *Curr. Opin. Biotechnol.* **2022**, *78*, 102785.

[4] L. H. L. Lua, N. K. Connors, F. Sainsbury, Y. P. Chuan, N. Wibowo, A. P. J. Middelberg, *Biotechnol. Bioeng.* **2014**, *111*, 425–440.
[5] A. Zeltins, *Mol. Biotechnol.* **2013**, *53*, 92–107.
[6] D. He, J. Marles-Wright, *New Biotechnol.* **2015**, *32*, 651–657.
[7] G. Jutz, P. van Rijn, B. S. Miranda, A. Böker, *Chem. Rev.* **2015**, *115*, 1653–1701.
[8] I. Stupka, J. G. Heddle, *Curr. Opin. Struct. Biol.* **2020**, *64*, 66–73.
[9] Y. Azuma, T. G. W. Edwardson, D. Hilvert, *Chem. Soc. Rev.* **2018**, *47*, 3543–3557.
[10] C. A. Kerfeld, C. Aussignargues, J. Zarzycki, F. Cai, M. Sutter, *Nat. Rev. Microbiol.* **2018**, *16*, 277–290.
[11] N. W. Kennedy, C. E. Mills, T. M. Nichols, C. H. Abrahamson, D. Tullman-Ercek, *Curr. Opin. Microbiol.* **2021**, *63*, 36–42.
[12] T. W. Giessen, *Annu. Rev. Biochem.* **2022**, *91*, 353–380.
[13] T. N. Szyszka, L. S. R. Adamson, Y. H. Lau, in *Microbial Production of High-Value Products* (Eds.: B.H.A. Rehm, D. Wibowo), Springer International Publishing, Cham, **2022**, pp. 309–333.
[14] Y. H. Lau, T. W. Giessen, W. J. Altenburg, P. A. Silver, *Nat. Commun.* **2018**, *9*, 1311.
[15] A. O'Neil, C. Reichhardt, B. Johnson, P. E. Prevelige, T. Douglas, *Angew. Chem. Int. Ed.* **2011**, *50*, 7425–7428.
[16] L. C. Cheah, T. Stark, L. S. R. Adamson, R. S. Abidin, Y. H. Lau, F. Sainsbury, C. E. Vickers, *ACS Synth. Biol.* **2021**, *10*, 3251–3263.
[17] Y. Azuma, D. Hilvert, in *Protein Scaffolds: Design, Synthesis, and Applications* (Ed.: A. K. Udit), Springer, New York, NY, **2018**, pp. 39–55.
[18] W. F. Rurup, J. Snijder, M. S. T. Koay, A. J. R. Heck, J. J. L. M. Cornelissen, *J. Am. Chem. Soc.* **2014**, *136*, 3828–3832.
[19] S. Tetter, D. Hilvert, *Angew. Chem. Int. Ed.* **2017**, *56*, 14933–14936.
[20] T. M. Nichols, N. W. Kennedy, D. Tullman-Ercek, in *Methods in Enzymology* (Eds.: C. Schmidt-Dannert, M. B. Quin), Academic Press, Cambridge, MA, United States, **2019**, pp. 155–186.
[21] T. Li, P. Chang, W. Chen, Z. Shi, C. Xue, G. F. Dykes, F. Huang, Q. Wang, L.-N. Liu, *ACS Nano* **2024**, *18*, 7473–7484.
[22] A. Van de Steen, H. C. Wilkinson, P. A. Dalby, S. Frank, *ACS Appl. Bio Mater.* **2024**, *7*, 3660–3674.
[23] I. Boyton, S. C. Goodchild, D. Diaz, A. Elbourne, L. E. Collins-Praino, A. Care, *ACS Omega* **2022**, *7*, 823–836.
[24] J. E. Glasgow, S. L. Capehart, M. B. Francis, D. Tullman-Ercek, *ACS Nano* **2012**, *6*, 8658–8664.
[25] V. Madigan, Y. Zhang, R. Raghavan, M. E. Wilkinson, G. Faure, E. Puccio, M. Segel, B. Lash, R. K. Macrae, F. Zhang, *Proc. Natl. Acad. Sci. USA* **2024**, *121*, e2307812120.
[26] M. Medrano, M. Á. Fuertes, A. Valbuena, P. J. P. Carrillo, A. Rodríguez-Huete, M. G. Mateu, *J. Am. Chem. Soc.* **2016**, *138*, 15385–15396.
[27] I. J. Minten, L. J. A. Hendriks, R. J. M. Nolte, J. J. L. M. Cornelissen, *J. Am. Chem. Soc.* **2009**, *131*, 17771–17773.
[28] A. Hebbelstrup, K. Teilum, *ChemistrySelect* **2024**, *9*, e202402826.
[29] H. Chen, S. Zhang, C. Xu, G. Zhao, *Chem. Commun.* **2016**, *52*, 7402–7405.
[30] E. Pascual, C. P. Mata, J. L. Carrascosa, J. R. Castón, *J. Phys.: Condens. Matter* **2017**, *29*, 494001.
[31] J. A. Jones, A. S. Cristie-David, M. P. Andreas, T. W. Giessen, *Angew. Chem. Int. Ed.* **2021**, *60*, 25034–25041.
[32] M. Comellas-Aragonès, H. Engelkamp, V. I. Claessen, N. A. J. M. Sommerdijk, A. E. Rowan, P. C. M. Christianen, J. C. Maan, B. J. M. Verduin, J. J. L. M. Cornelissen, R. J. M. Nolte, *Nat. Nanotechnol.* **2007**, *2*, 635–639.
[33] K. W. Lee, W. S. Tan, *J. Virol. Methods* **2008**, *151*, 172–180.
[34] D. McNeale, N. Dashti, L. C. Cheah, F. Sainsbury, *WIREs Nanomed. Nanobiotechnol.* **2023**, *15*, e1869.
[35] Y. Hu, R. Zandi, A. Anavitarte, C. M. Knobler, W. M. Gelbart, *Biophys. J.* **2008**, *94*, 1428–1436.
[36] K. W. Lee, W. S. Tan, *J. Virol. Methods* **2008**, *151*, 172–180.
[37] A. A. A. Aljabali, F. Sainsbury, G. P. Lomonossoff, D. J. Evans, *Small* **2010**, *6*, 818–821.
[38] M. Ruszkowski, A. Strugala, P. Indyka, G. Tresset, M. Figlerowicz, A. Urbanowicz, *Nanoscale* **2022**, *14*, 3224–3233.
[39] K. Bond, I. B. Tsvetkova, J. C.-Y. Wang, M. F. Jarrold, B. Dragnea, *Small* **2020**, *16*, 2004475.
[40] H. Moon, J. Lee, J. Min, S. Kang, *Biomacromolecules* **2014**, *15*, 3794–3801.
[41] D. Diaz, X. Vidal, A. Sunna, A. Care, *ACS Appl. Mater. Interfaces* **2021**, *13*, 7977–7986.
[42] C. Rennie, C. Sives, I. Boyton, D. Diaz, C. Gorrie, O. Vittorio, L. Collins-Praino, A. Care, *Adv. Therap.* **2024**, *7*, 2300360.
[43] P. Lagoutte, C. Mignon, G. Stadthagen, S. Potisopon, S. Donnat, J. Mast, A. Lugari, B. Werle, *Vaccine* **2018**, *36*, 3622–3628.
[44] M. C. Jenkins, S. Lutz, *ACS Synth. Biol.* **2021**, *10*, 857–869.
[45] E. M. Williams, S. M. Jung, J. L. Coffman, S. Lutz, *ACS Synth. Biol.* **2018**, *7*, 2514–2517.
[46] C. Cassidy-Amstutz, L. Oltrogge, C. C. Going, A. Lee, P. Teng, D. Quintanilla, A. East-Seletsky, E. R. Williams, D. F. Savage, *Biochemistry* **2016**, *55*, 3461–3468.
[47] T. W. Giessen, B. J. Orlando, A. A. Verdegaal, M. G. Chambers, J. Gardener, D. C. Bell, G. Birrane, M. Liao, P. A. Silver, *eLife* **2019**, *8*, e46070.
[48] J. A. Cotruvo Jr., E. R. Featherston, J. A. Mattocks, J. V. Ho, T. N. Laremore, *J. Am. Chem. Soc.* **2018**, *140*, 15056–15061.
[49] J. A. Jones, A. S. Cristie-David, M. P. Andreas, T. W. Giessen, *Angew. Chem. Int. Ed.* **2021**, *60*, 25034–25041.
[50] S. Kwon, M. P. Andreas, T. W. Giessen, *J. Struct. Biol.* **2023**, *215*, 108022.
[51] R. M. Putri, C. Allende-Ballestero, D. Luque, R. Klem, K.-A. Rousou, A. Liu, C. H.-H. Traulsen, W. F. Rurup, M. S. T. Koay, J. R. Castón, *ACS Nano* **2017**, *11*, 12796–12804.
[52] P. Lohner, M. Zmyslia, J. Thurn, J. K. Pape, R. Gerasimaitė, J. Keller-Findeisen, S. Groeer, B. Deuringer, R. Süss, A. Walther, S. W. Hell, G. Lukinavičius, T. Hugel, C. Jessen-Trefzer, *Angew. Chem.* **2021**, *133*, 24028–24034.
[53] H. H. Gustafson, D. Holt-Casper, D. W. Grainger, H. Ghandehari, *Nano Today* **2015**, *10*, 487–510.
[54] F. Toscano, M. Torres-Arias, *Curr. Res. Immunol.* **2023**, *4*, 100073.
[55] D. McNeale, L. Esquirol, S. Okada, S. Strampel, N. Dashti, B. Rehm, T. Douglas, C. Vickers, F. Sainsbury, *ACS Appl. Mater. Interfaces* **2023**, *15*, 17705–17715.
[56] N. H. Dashti, R. S. Abidin, F. Sainsbury, *ACS Nano* **2018**, *12*, 4615–4623.
[57] F. Lie, T. N. Szyszka, Y. H. Lau, *J. Mater. Chem. B* **2023**, *11*, 6516–6526.
[58] W. F. Rurup, F. Verbij, M. S. T. Koay, C. Blum, V. Subramaniam, J. J. L. M. Cornelissen, *Biomacromolecules* **2014**, *15*, 558–563.
[59] J. Escrig, í. Marcos-Alcalde, S. Domínguez-Zotes, D. Abia, P. Gómez-Puertas, A. Valbuena, M. G. Mateu, *ACS Nano* **2024**, *18*, 27465–27478.
[60] C. B. Chang, C. M. Knobler, W. M. Gelbart, T. G. Mason, *ACS Nano* **2008**, *2*, 281–286.
[61] L. S. R. Adamson, N. Tasneem, M. P. Andreas, W. Close, E. N. Jenner, T. N. Szyszka, R. Young, L. C. Cheah, A. Norman, H. I. MacDermott-Opeskin, M. L. O'Mara, F. Sainsbury, T. W. Giessen, Y. H. Lau, *Sci. Adv.* **2022**, *8*, eabl7346.
[62] S. A. Bode, I. J. Minten, R. J. M. Nolte, J. J. L. M. Cornelissen, *Nanoscale* **2011**, *3*, 2376.
[63] D. P. Patterson, P. E. Prevelige, T. Douglas, *ACS Nano* **2012**, *6*, 5000–5009.

[64] M. Brasch, R. M. Putri, M. V. de Ruiter, D. Luque, M. S. T. Koay, J. R. Castón, J. J. L. M. Cornelissen, *J. Am. Chem. Soc.* **2017**, *139*, 1512–1519.
[65] I. J. Minten, V. I. Claessen, K. Blank, A. E. Rowan, R. J. M. Nolte, J. J. L. M. Cornelissen, *Chem. Sci.* **2011**, *2*, 358–362.
[66] T.-H. Lee, T. S. Carpenter, P. D'haeseleer, D. F. Savage, M. C. Yung, *Biotechnol. Bioeng.* **2020**, *117*, 603–613.
[67] F. Akita, K. T. Chong, H. Tanaka, E. Yamashita, N. Miyazaki, Y. Nakaishi, M. Suzuki, K. Namba, Y. Ono, T. Tsukihara, A. Nakagawa, *J. Mol. Biol.* **2007**, *368*, 1469–1483.
[68] M. M. Suhanovsky, C. M. Teschke, *Virology* **2015**, *479-480*, 487–497.
[69] M. Cuillel, C. Berthet-Colominas, P. A. Timmins, M. Zulauf, *Eur. Biophys. J.* **1987**, *15*, 169–176.
[70] M. G. M. van Rosmalen, C. Li, A. Zlotnick, G. J. L. Wuite, W. H. Roos, *Biophys. J.* **2018**, *115*, 1656–1665.
[71] A. R. Hagen, J. S. Plegaria, N. Sloan, B. Ferlez, C. Aussignargues, R. Burton, C. A. Kerfeld, *Nano Lett.* **2018**, *18*, 7030–7037.
[72] M. Hori, A. Steinauer, S. Tetter, J. Hälg, E.-M. Manz, D. Hilvert, *Nat. Commun.* **2024**, *15*, 3576.
[73] L. Kavčič, A. Kežar, N. Koritnik, M. T. Žnidarič, T. Klobučar, Ž. Vičič, F. Merzel, E. Holden, J. L. P. Benesch, M. Podobnik, *Commun. Chem.* **2024**, *7*, 1–19.
[74] N. C. Shaner, G. G. Lambert, A. Chammas, Y. Ni, P. J. Cranfill, M. A. Baird, B. R. Sell, J. R. Allen, R. N. Day, M. Israelsson, *Nat. Methods* **2013**, *10*, 407–409.

Manuscript received: November 18, 2024
Revised manuscript received: March 26, 2025
Accepted manuscript online: March 26, 2025
Version of record online: May 07, 2025